

Measurement of the Difference in $R = \sigma_L/\sigma_T$ and of σ^A/σ^D in Deep-Inelastic e -D, e -Fe, and e -Au Scattering

S. Dasu,⁽¹⁾ P. de Barbaro,⁽¹⁾ A. Bodek,⁽¹⁾ H. Harada,⁽¹⁾ M. W. Krasny,⁽¹⁾ K. Lang,⁽¹⁾ E. M. Riordan,⁽¹⁾ R. Arnold,⁽²⁾ D. Benton,⁽²⁾ P. Bosted,⁽²⁾ L. Clogher,⁽²⁾ G. deChambrier,⁽²⁾ A. Lung,⁽²⁾ S. E. Rock,⁽²⁾ Z. M. Szalata,⁽²⁾ R. C. Walker,⁽³⁾ B. W. Filippone,⁽³⁾ J. Jourdan,⁽³⁾ R. Milner,⁽³⁾ R. McKeown,⁽³⁾ D. Potterveld,⁽³⁾ A. Para,⁽⁴⁾ F. Dietrich,⁽⁵⁾ K. Van Bibber,⁽⁵⁾ J. Button-Shafer,⁽⁶⁾ B. Debebe,⁽⁶⁾ R. S. Hicks,⁽⁶⁾ R. Gearhart,⁽⁷⁾ L. W. Whitlow,⁽⁸⁾ and J. Alster⁽⁹⁾

⁽¹⁾University of Rochester, Rochester, New York 14627

⁽²⁾The American University, Washington, DC 20016

⁽³⁾California Institute of Technology, Pasadena, California 91125

⁽⁴⁾Fermi National Accelerator Laboratory, Batavia, Illinois 60510

⁽⁵⁾Lawrence Livermore National Laboratory, Livermore, California 94550

⁽⁶⁾University of Massachusetts, Amherst, Massachusetts 01003

⁽⁷⁾Stanford Linear Accelerator Center, Stanford, California 94305

⁽⁸⁾Stanford University, Stanford, California 94305

⁽⁹⁾University of Tel-Aviv, Ramat Aviv, Tel-Aviv 69978, Israel

(Received 2 February 1988)

We measured the differences in $R = \sigma_L/\sigma_T$ and the cross-section ratio σ^A/σ^D in deep-inelastic electron scattering from D, Fe, and Au nuclei in the kinematic range $0.2 \leq x \leq 0.5$ and $1 \leq Q^2 \leq 5$ (GeV/c)². Our results for $R^A - R^D$ are consistent with zero for all x and Q^2 , indicating that possible contributions to R from nuclear higher-twist effects and spin-0 constituents in nuclei are not different from those in nucleons. The European Muon Collaboration effect is reconfirmed, and the low- x data from all recent experiments, at all Q^2 , are now in agreement.

PACS numbers: 25.30.Fj, 12.38.Qk, 13.60.Hb

The discovery of the difference in the deep-inelastic cross sections for iron and deuterium targets,¹⁻⁴ known as the European Muon Collaboration (EMC) effect, has sparked considerable activity in the theoretical study of deep-inelastic lepton scattering from nuclear targets. There are numerous models⁵ for the EMC effect which are built on a variety of ideas (a swelling of nucleons bound in a nucleus, the presence of tightly bound pions, Δ isobars, multi-quark clusters, etc., in nuclei, and others) which result in a change of quark distributions in nuclei compared with those in free nucleons. The less drastic models attribute the EMC effect to nuclear-binding corrections alone. To compare the theoretical predictions for the structure-function ratio with the experimental results on the cross-section ratio, it is essential to measure the differences in $R = \sigma_L/\sigma_T$, the ratio of longitudinal (σ_L) and transverse (σ_T) virtual-photon absorption cross sections. Some models⁶ predict a large difference in the quantity R for deuterium and iron ($R^{\text{Fe}} - R^{\text{D}} \approx 0.1-0.15$). Others,^{5,7} including those based on quantum chromodynamics (QCD), predict a

negligible difference ($R^{\text{Fe}} - R^{\text{D}} \approx 0.002$). Some authors⁸ have conjectured that higher-twist effects might be different for different nuclei, and yield an atomic-mass (A) dependence of R . The quantity R is a sensitive measure of pointlike spin-0 constituents (e.g., tightly bound diquarks) of the nucleus. Therefore an A dependence of R could alter our view of nuclear structure in terms of spin- $\frac{1}{2}$ quarks and vector gluons. The large initial discrepancy at low x between σ^A/σ^D as measured at CERN¹ (European Muon Collaboration) and at SLAC²⁻⁴ at different angles and energies could have been due to either a Q^2 dependence, a value⁹ of $R^{\text{Fe}} - R^{\text{D}} \approx 0.15$, or an experimental uncertainty. There were indications in previous data³ (SLAC E139) that such a difference in R may have been observed.

We have undertaken precision measurements of deep-inelastic electron-scattering cross sections on deuterium, iron, and gold targets, to resolve these questions. The differential cross section for scattering of an unpolarized charged lepton with an incident energy E , scattering angle θ , and final energy E' can be written in terms of structure functions F_1 and F_2 as

$$\begin{aligned} d^2\sigma(E, E', \theta)/d\Omega dE' &= (4\alpha^2 E'^2/Q^4) \cos^2(\frac{1}{2}\theta) [F_2(x, Q^2)/\nu + 2 \tan^2(\frac{1}{2}\theta) F_1(x, Q^2)/M] \\ &= \Gamma \sigma_T(x, Q^2) [1 + \epsilon R(x, Q^2)], \end{aligned} \quad (1)$$

where α is the fine-structure constant, M is the nucleon mass, $\nu = E - E'$ is the energy of the virtual photon which mediates the interaction, $Q^2 = 4EE' \sin^2(\frac{1}{2}\theta)$ is the invariant four-momentum transfer squared, and the variable $x = Q^2/2M\nu$ is a measure of the longitudinal momentum carried by struck nucleon constituents. In Eq. (1) the differential

cross section is also related to R , with

$$\Gamma = \frac{\alpha}{4\pi^2} \frac{(2Mv - Q^2)E'}{Q^2ME} \left(\frac{1}{1 - \epsilon} \right)$$

and $\epsilon = [1 + 2(1 + v^2/Q^2)\tan^2(\frac{1}{2}\theta)]^{-1}$ representing the virtual-photon flux and polarization, respectively. R can also be expressed as $R = F_L/2xF_1$, where the longitudinal structure function $F_L = (1 + 4M^2x^2/Q^2)F_2 - 2xF_1$ is proportional to σ_L . Within the parton models and QCD, contributions to F_L originate from gluon emission, target mass effects,¹⁰ and pointlike spin-0 constituents. The structure function $2xF_1(x)$ is equal to $\sum_i e_i^2[xq_i(x, Q^2) + x\bar{q}_i(x, Q^2)]$, where $xq_i(x, Q^2)$ and $x\bar{q}_i(x, Q^2)$ are quark and antiquark momentum distributions, and e_i is the quark electric charge for the i th flavor. In this paper the *differential* cross sections *per average nucleon* (including the correction for neutron excess in Fe and Au) are represented as σ^A for Fe and Au and σ^D for D.

The electron beams and the 8-GeV spectrometer facility, at the Stanford Linear Accelerator Center (SLAC), are uniquely suited for a measurement of R , because deep-inelastic cross sections can be measured to better than $\pm 1\%$ over a wide range of ϵ at various x and Q^2 . In this experiment the SLAC beam was tuned over a broad energy range (between 3.75 and 19.5 GeV) with a precision of $\pm 0.1\%$. A single spectrometer with fixed acceptance was used to detect electrons by varying scattered momenta and angles between 1 and 8 GeV, and 11° and 46° , respectively. The kinematic region was limited by the background levels, counting rates, and the size of radiative corrections to the x, Q^2 range of $0.2 \leq x \leq 0.5$ and $1 \leq Q^2 \leq 10$ (GeV/c)². Cross sections were measured, for each (x, Q^2) point, at up to five different values of ϵ (with a typical ϵ range of 0.35) on targets of liquid D₂ [2.6% radiation lengths (r.l.)], Fe (2.6% and 6% r.l.), and Au (6% r.l.). Values of R for each target have been extracted from these measurements and will be presented in a future communication. The results for the difference $R^A - R^D$ and the ratio σ^A/σ^D have smaller systematic errors and are presented here.

Accurate determination of cross sections demanded careful monitoring of the apparatus during data taking. For the σ^A/σ^D and $R^A - R^D$ measurements, the stability of data-taking conditions and the differences between running conditions for the liquid D₂ and Fe targets were crucial. Extensive measures were taken to minimize systematic errors (summarized in Table I). The beam position and angle were continuously monitored and controlled. The total incident charge was measured with two precision toroidal charge monitors, which were frequently calibrated during the experiment. Errors arising from any time-dependent fluctuations were reduced by the accumulation of the data in small runs alternating between various targets. The liquid target assembly con-

TABLE I. Typical systematic errors on σ^A/σ^D and $R^A - R^D$.

Source	Uncertainty A or D	Error (\pm)	
		σ^A/σ^D	$R^A - R^D$
Beam steering	0.003°	0.1%	0.004
Incident energy	0.1%	0.3%	0.014
Charge measurement	0.1%	0.1%	0.004
D target density	0.2%	0.2%	0.010
D acceptance	0.1%	0.1%	0.004
e^+/e^- background	0.1%	0.1%	0.004
A neutron excess	0.2%	0.2%	...
Total point to point		0.4%	0.019
Target length error	0.5%–1.5%	1.0%	...
Radiative corrections	0.5%	0.5%	0.015

sisted of an aluminum tube through which liquid D₂ flowed continuously. The liquid-D₂ pressure and temperature (and hence average density) were measured continuously. A new detector package was used to attain an electron-detection efficiency of 99.5% while maintaining pion misidentification level below 10^{-5} . It included an upgraded hydrogen-gas Cherenkov counter, a ten-plane proportional wire chamber system, a new five-layer lead-glass shower-counter array, and three planes of plastic scintillation counters. The ratio of yields π/e was less than 120 (π contamination $< 0.1\%$) and was the same within a factor of 2 for Fe and D targets, at all the kinematic settings. The flux of electrons from processes¹¹ other than deep-inelastic scattering was measured and subtracted.

Radiative corrections to deep-inelastic electron scattering can be separated into two distinct contributions.¹² The corrections to high-momentum-transfer scattering process due to vacuum polarization, vertex correction, and photon emission are called “internal.” The corrections due to electron energy loss in traversing the target material due to bremsstrahlung and ionization are called “external.” The “internal” corrections were calculated with the prescription of Bardin.¹³ These did not differ by more than 1% between the deuterium and solid targets. The “external” effects, calculated in accord to the prescription of Mo and Tsai,¹² are strongly dependent on the target radiation lengths and hence are different for the Fe and D targets. Significant improvements¹⁴ have been made by use of the complete formalism rather than the energy-peaking approximation expressions derived by Tsai. The cross sections and the values of R obtained for targets of different radiation lengths were compared to test the calculations of the radiative corrections. The values of R extracted from the 2.6% and 6% Fe-target data of this experiment were the same within statistical errors ($(R^{\text{Fe6}} - R^{\text{Fe2.6}}) = -0.040 \pm 0.042$). The average ratio of the cross sections $\sigma^{\text{Fe6}}/\sigma^{\text{Fe2.6}}$ was $1.017 \pm 0.005 \pm 0.020$. In addition, radi-

TABLE II. Values of $R^A - R^D$, and σ^A/σ^D averaged over ϵ with statistical (stat.) and point-to-point systematic (syst.) errors. There is an additional error of ± 0.015 in $R^A - R^D$ because of radiative corrections and an overall normalization error (Δ) in σ^A/σ^D of $\pm 1.1\%$.

Target	r.l.	x	Q^2	$\Delta\epsilon'$	Value	$R^A - R^D$		Value	σ^A/σ^D	
						Stat.	Syst.		Stat.	Syst.
Fe	2.6	0.20	1.00	0.24	-0.040	0.059	0.021	1.006	0.005	0.004
Fe	6.0	0.20	1.00	0.24	-0.084	0.058	0.020	1.022	0.005	0.004
Au	6.0	0.20	1.00	0.24	-0.042	0.060	0.021	1.021	0.005	0.004
Fe	6.0	0.20	1.50	0.23	-0.140	0.057	0.018	1.028	0.004	0.002
Fe	6.0	0.20	2.50	0.33	0.141	0.075	0.025	1.023	0.006	0.002
Fe	6.0	0.35	1.50	0.20	0.037	0.080	0.027	1.000	0.005	0.002
Fe	6.0	0.35	2.50	0.28	0.104	0.055	0.019	0.995	0.005	0.002
Fe	6.0	0.35	5.00	0.28	0.023	0.059	0.016	0.981	0.005	0.002
Fe	2.6	0.50	2.50	0.37	0.040	0.059	0.016	0.923	0.009	0.005
Fe	6.0	0.50	2.50	0.37	0.021	0.038	0.014	0.933	0.005	0.002
Fe	6.0	0.50	5.00	0.39	-0.018	0.050	0.017	0.939	0.006	0.004

ative corrections for SLAC E139 data with 12% (unpublished), 6% and 2% r.l. Fe targets³ were calculated. The cross sections for 12% r.l. data agreed with 2% and 6% data at all kinematics only after the application of the improved radiative corrections. We have therefore applied the improved radiative corrections to the SLAC E139 data as well. These SLAC E139 results are higher than the peaking approximation results³ by about 1%. The improvements in "external" corrections did not affect the $\sigma^{\text{Fe}}/\sigma^D$ results of SLAC E87² and SLAC E61⁴ data, since those experiments used D and Fe targets of equal radiation lengths.

The difference $R^A - R^D$ was determined by our making linear fits, weighted by the statistical and point-to-point (ϵ -uncorrelated) systematic errors, to the ratio of cross sections,

$$\sigma^A/\sigma^D = F_A^A/F_D^D [1 + \epsilon'(R^A - R^D)],$$

versus $\epsilon' = \epsilon/(1 + \epsilon R^D)$. The $R^A - R^D$ results are thus independent of absolute normalizations of target length, spectrometer acceptance, beam intensity, and energy scale. They are also insensitive to changes in acceptance with ϵ , offsets in beam energy, spectrometer angle, survey errors, long-term charge-monitor drifts, and "internal" radiative corrections. The values of $R^A - R^D$ for all (x, Q^2) points are shown in Table II. The average χ^2 per degree of freedom for the goodness of fit was 0.7 indicating that the estimate of systematic uncertainty is conservative. The results are also plotted against x for various Q^2 values in Fig. 1(a). Our results for $R^A - R^D$ show no x or Q^2 dependence, and are consistent with zero at all measured values. The average value is $\langle R^A - R^D \rangle = 0.001 \pm 0.018$ (statistical) ± 0.016 (systematic).

The results for the ratio σ^A/σ^D averaged over various ϵ points are also shown in Table II. The overall normalization error (Δ) in σ^A/σ^D of $\Delta = \pm 1.1\%$ is dominated by the errors in target length¹⁵ measurement and radiative corrections. Our results for σ^A/σ^D averaged over Q^2

and ϵ are compared with data from SLAC E139 (with improved radiative corrections, $\Delta = \pm 1.3\%$),³ SLAC E87 ($\Delta = \pm 1.1\%$),² and SLAC E61 ($\Delta = \pm 4.2\%$)⁴ in

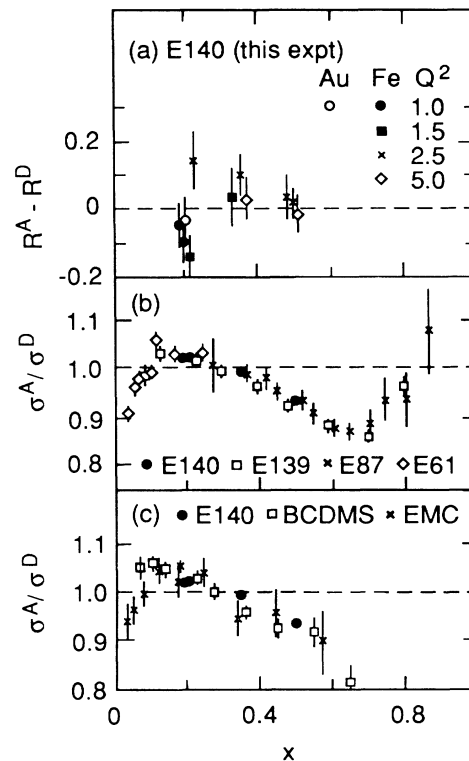


FIG. 1. (a) The results for $R - R^D$ are plotted as functions of x ; 2.6% and 6% Fe, and Au (open symbol) targets are plotted separately. Statistical and systematic errors are added in quadrature. (b),(c) The results for σ^A/σ^D are plotted as functions of x and are compared with other (b) electron and (c) muon experiments. Our data from Fe and Au ($x=0.2$) targets are each averaged over ϵ and Q^2 . Statistical and point-to-point systematic errors are added in quadrature for all experiments. The overall normalization errors (Δ) are discussed in text.

Fig. 1(b). There is excellent agreement between all the SLAC data. In Fig. 1(c) our data are compared with high- Q^2 data from CERN muon experiments by the Bologna-CERN-Dubna-Munich-Saclay (BCDMS) collaboration ($\Delta = \pm 1.5\%$),¹⁶ and the EMC (preliminary results, $\Delta = \pm 0.8\%$).¹⁷ The initial low- x discrepancy between EMC and SLAC data is now resolved.

We conclude that $R^A - R^D$ is consistent with zero, in agreement with models which predict no A dependence of R (e.g., QCD). We rule out models⁶ predicting a large difference $R^A - R^D$. Our data indicate that possible contributions to R from nuclear higher-twist effects and spin-0 constituents in nuclei are not different from those in nucleons. The σ^A/σ^D measurements can now be identified with the structure-function ratios F_2^A/F_2^D and F_1^A/F_1^D . The EMC effect is confirmed with very small errors and all recent data are now in agreement. The ratio σ^A/σ^D is larger than unity at low x , and is therefore inconsistent with models using nuclear-binding corrections only. Because the ratio F_1^A/F_1^D is equal to the ratio of quark distribution functions, we conclude that the EMC effect is due to a nontrivial difference in the quark distributions between heavy nuclei and the deuteron.^{5,7}

We acknowledge the support of Professor B. Richter and the SLAC staff, which was crucial for the success of this experiment. This research was supported by Department of Energy Contracts No. DE-AC02-76ER13065, No. DE-AC02-76ER02853, No. DE-AC03-96SF00515, and No. W-7405-ENG-48, and National Science Foundation Contracts No. PHY84-10549 and No. PHY85-05682.

¹J. J. Aubert *et al.*, Phys. Lett. **123B**, 275 (1983); G. Bari *et al.*, Phys. Lett. **163B**, 282 (1985).

²A. Bodek *et al.*, Phys. Rev. Lett. **50**, 1431 (1983), and **51**, 534 (1983).

³R. G. Arnold *et al.*, Phys. Rev. Lett. **52**, 727 (1984), and SLAC Report No. SLAC-PUB-3257, 1983 (unpublished).

⁴S. Stein *et al.*, Phys. Rev. D **12**, 1884 (1975).

⁵E. Berger and F. Coester, Annu. Rev. Nucl. Part. Sci. **37**, 463 (1987).

⁶Bo-Qiang Ma and Ji Sun, Beijing University Report No. Print-86-1217, 1986 (unpublished).

⁷F. E. Close *et al.*, Phys. Lett. **129B**, 346 (1983) (QCD model); R. D. Smith, Phys. Lett. B **182**, 283 (1986) (convolution model).

⁸E. V. Shuryak, Nucl. Phys. **A446**, 259C (1985).

⁹I. A. Savin and G. I. Smirnov, Phys. Lett. **145B**, 438 (1984).

¹⁰A. De Rújula *et al.*, Ann. Phys. **103**, 315 (1977); G. Altarelli and G. Martinelli, Phys. Lett. **76B**, 89 (1978).

¹¹L. S. Rochester *et al.*, Phys. Rev. Lett. **36**, 1284 (1976).

¹²L. W. Mo and Y. S. Tsai, Rev. Mod. Phys. **41**, 205 (1969); Y. S. Tsai, SLAC Report No. SLAC-PUB-848, 1971 (unpublished); equation (C.1) from SLAC-PUB-848 was used to calculate the "external" effects. The shape of the internal bremsstrahlung was approximated by that of the external bremsstrahlung (i.e., the method of equivalent radiators) in the evaluation of this double integral.

¹³D. Y. Bardin and N. M. Shumeiko, Yad. Phys. **29**, 499 (1979) [Sov. J. Nucl. Phys. **29**, 969 (1979)]; D. Y. Bardin *et al.*, Nucl. Phys. **B 197**, 1 (1982), and references therein.

¹⁴S. Dasu, Ph.D. thesis, University of Rochester Report No. UR-1059, 1988 (unpublished).

¹⁵Uncertainties on the target lengths are $\pm 0.5\%$ for D and Fe 6% r.l. targets, and $\pm 1.5\%$ for the Fe 2.6% r.l. and Au 6% r.l. targets.

¹⁶A. C. Benvenuti *et al.*, Phys. Lett. **B 189**, 483 (1987).

¹⁷M. Dueren, in *Proceedings of the International Europhysics Conference on High Energy Physics, Uppsala, Sweden, 1987*, edited by O. Botner (European Physical Society, Switzerland, 1987).